The *in-situ* Evaluation of Surface-Breaking Cracks in Asphalt Using a Wave Decomposition Method

M Iodice, J M Muggleton and E Rustighi

Institute of Sound and Vibration Research, University of Southampton; Southampton, United Kingdom

E_mail: michele.iodice@gmail.com

Tel. No.: +44(0)7767715748

Abstract: Assessment of the location and extension of cracking in road surfaces is important for determining the potential level of deterioration in the road and in the infrastructure buried beneath it. Damage in a pavement structure is usually initiated in the asphalt layers, making the Rayleigh wave ideally suited to the detection of shallow surface defects. However, the practical application of crack detection methods in asphalt is hampered by the dispersive behaviour of the road pavement. In fact, assessment of crack in road is usually performed assuming constant phase velocity, and its dispersive behaviour is neglected. Moreover, current methodologies for crack evaluation in asphalt do not support *in-situ* applications. A new digital signal processing technique for the measurement of the amplitude and phase of the direct and reflected Rayleigh waves, scattered from the boundaries of a vertical crack in asphalt, is presented in this paper for the first time. It decomposes the signal into its

direct and reflected components. The method uses multiple receivers and hence it finds an approximate solution with a least square optimization. The resonant peak frequencies of the reflection coefficient and the cut-off frequencies of the transmission coefficient are used for assessing the depth of the crack. The study is conducted through numerical simulations alongside experimental investigations and it considers the cases for which the cracking is internal or external to the deployment of sensors. The method proved to be successful for the *in-situ* assessment of the depth of cracks both numerically and experimentally, since it can cope with the dispersive and heterogeneous nature of asphalt. This work supports a paradigm-shifting approach to *in-situ* crack evaluation of roads, for which the road is holistically treated as a dispersive medium.

Keywords: cracks, asphalt, reflection coefficient, transmission coefficient, wave decomposition, dispersion, overdetermined system.

1. Introduction

Paved roads provide a smooth and regular surface for vehicles to move along easily and safely. The structure of the paved road usually consists of a multi-layered system of bitumen-bound and unbound materials disposed on top of each other, constituting in fact a dispersive system. The main purpose of the layers is to distribute traffic loads from the vehicles to the underlying natural soil.

The routinely investigation of the structural integrity of the road network is of primary importance [1]. The budget allocated for engineering maintenance of highways in England in

2017 was of £3.05 billion. This number is expected to grow in the next years to address the backlog in the maintenance and the increasing deterioration of the road network [2].

One of the ways in which damage in a pavement road structure manifests itself are cracks, which are most commonly initiated in the asphalt layers. This makes Rayleigh wave (R-wave) ideally suited for the detection of shallow surface defects through efficient non-destructive techniques (NDTs). The proper assessment of the location and of the extension of such discontinuities is crucial for the determination of the level of deterioration of an infrastructure and for decisions regarding maintenance, strengthening and rebuilding of existing infrastructures.

Many researchers have approached the detection and evaluation of cracks in asphalt quantitatively, by monitoring the asphalt stiffness over time [1], [3]–[9]. They all converged to the same general conclusion that a drop of about 30% in the initial value of the stiffness modulus of asphalt (i.e. at the beginning of the infrastructure's service life) is a signal of incipient failure, or in other words the beginning of the phenomenon of fractures. The most common methods for the calculation of layers' stiffness using R-wave are the Multichannel Analysis of Surface Waves (MASW), the Multiple Impact of Surface Waves (MISW) and the Multichannel Simulation with One Receiver (MSOR). They all share two basic steps: the measure of an experimental dispersion curve and the estimation of a layer model by matching the measured dispersion curve with a theoretical dispersion curve (inversion) [1], [10]–[12]. Researchers observed that cracked specimens of asphalt have a peculiar acoustic spectrum, which can be exploited to infer the overall current pavement condition and monitor it over time [13]. Although it seems possible to measure the residual life of an infrastructure by

monitoring the stiffness or acoustic spectra over time, there are significant challenges still to be addressed. For example, a reference value of the stiffness for every different asphalt mixture is required. Adding to the problem complexity is the fact that the influences of temperature and self-repairing mechanisms ongoing in an asphalt pavement during its life are yet to be understood, and that seismic methods for monitoring asphalt deterioration should be able to cope with the inhomogeneity, anisotropy and dispersive nature of the road layers.

An overview of the current state-of-the-art in the evaluation of the depth of surface-breaking cracks in non-dispersive materials, like concrete and metals, is essential to understand the challenges when evaluating cracks on dispersive media. Two main approaches are conventionally pursued: time-of-flight based approaches (in the time domain) and frequency based approaches (in the frequency domain) [14]. Time-of-flight methods are based on the estimation of the time required for a longitudinal wave to travel from the location it was originated, to the opposite side of the crack, travelling across the tip of the surface-breaking crack [14]. These methods are explored by many authors as a tool for crack interrogation, and they proved to be accurate when applied to real structures [7], [14]–[18].

On the other hand, frequency based methods rely on the analysis of data in the frequency domain after some types of transformation (e.g. Fourier, Wavelet, frequency-wavenumber). The vertical crack has a resonance-type feature which occurs periodically at certain frequencies and has found to be associated with the depths of the cracks [16], [19]–[21]. Moreover the edges of free surface defects (like cracks) act like a source that excites surface waves which propagate along the crack surface [15], [20]. The finite depth of the surface-breaking crack blocks the shorter wavelengths, allowing only the longer wavelengths to

proceed, and hence acting as a low-pass filter. The reflections and the changes in the frequency bandwidth of a seismic signal at the surface, caused by the presence of the crack, are exploited for its detection and evaluation[22], [23].

Particularly, the resonant effects of the scattering waves [20] or leaky Rayleigh waves [16] in the ultrasonic range of frequencies are exploited to extract the information about the depth and the length of a surface crack. Wave transmission, reflection and attenuation spectral ratios are often exploited by various authors for detection and sizing of surface discontinuities [7], [14], [24]–[27], exploiting the resonant features of surface-breaking cracks. Spectral analysis of acoustic emission is also exploited by many for crack evaluation and localization [22]–[24], [28]–[30]. The use of the frequency-wavenumber spectral images, sometimes combined with the power spectral density, obtained from an array of sensors both numerically and experimentally, proved to be a successful tool for the assessment of the crack depth, but inaccurate for its location, [24], [28], [30]. A time-frequency analysis of the acoustic emission, based on the wavelet transform, is also exploited numerically for big anomalies detection in layered media [22], and for cracks detection in laboratory specimens [29].

Despite frequency based and time-of-flight based methods showed to be often successful, at various degrees, in estimating the depth of surface cracks in non-dispersive materials, the practical, reliable, *in-situ* evaluation of cracks in asphalt needs to take into account the heterogeneous nature of the materials tested and its dispersive behaviour, which inevitably make these methods dependent on the wavespeed at different depths and frequencies. Besides, the current state-of-the-art in the evaluation of cracks in asphalt with acoustic methods are based on the detection of very shallow, top-down cracks in homogeneous, non-

dispersive, monochromatic, single-mode, single-layered slabs or specimens, or on the assumption of constant velocity at ultrasonic frequencies [17], [18], [27]. Current methods deliberately neglect the complex, dispersive, inhomogeneous, multi-mode, layered features of the road system and do not support *in-situ* applications. They do not investigate bottom-up cracks. Simplistic approaches to crack evaluation in dispersive media lead to troublesome crack detection strategies [31].

In this paper, a digital signal processing algorithm for the *in-situ* detection and assessment of vertical surface-breaking cracks in asphalt layers is developed. Its accuracy is investigated with the aid of numerical and experimental investigations. The new method overcomes the aforementioned contradictions and limitations in computing the reflection and the transmission coefficients in dispersive media. Particularly, it copes with the dispersive and heterogeneous nature of materials, by magnifying the results of the frequency-wavenumber (*f-k*) transformation with the wave decomposition method. The decomposition of the wave is provided by filtering the outputs of an array of sensors: a similar technique is currently applied to wave-guided systems as beams and pipes, using two receivers [32], [33]. The assumption of constant phase velocity of asphalt layers and the assumption of non-dispersive behaviour, are lifted, supporting a paradigm-shifting approach to the assessment of surface-breaking crack in roads. In this work, the road system is considered holistically as a dispersive medium. The proposed wave decomposition method allows for the assessment of depth of vertical discontinuities, by knowing the amplitude of the positive and of the negative going Rayleigh wave components propagating in the top layers of a complex system, i.e. the road pavement system. Particularly, the resonant peak frequencies of the reflection coefficient and the cut-

off frequencies of the transmission coefficient give the information about the depth of a vertical discontinuity.

The rationale belonging to the new wave decomposition method is introduced and explained in section 2. Section 3 describes the two-dimensional model assembled with the Finite Element Method (FEM) to numerically test the wave decomposition method. As a proof of concept, only big, wide, top-down cracks are considered in this paper. The numerical simulations of section 4 complement the analytical explanation and show the benefits of the new method. Section 5 illustrates the outcome of the wave decomposition method applied on data coming from two experimental investigations. Finally, section 6 describes a strategy for crack interrogation and section 7 draws the conclusions.

2. The wave decomposition method

A new technique for the measurement of the amplitude and phase of the direct and reflected surface wave from a vertical discontinuity in asphalt layers is proposed.

The wave decomposition test set-up comprises a set of two or more receivers (e.g. geophones), disposed on the road surface with an equal spacing along a survey line, and a source of seismic energy (e.g. a shaker or an impact hammer), as shown in Figure 1. It is noteworthy that the set-up is the same routinely used for MASW testing. According to Figure 1, in the case of a two-receivers' set-up and for the mono-dimensional case, the amplitude of the signal at two different locations (R_1) and (R_2) can be written as:

$$\begin{cases} U(R_1) = r^{-}e^{+ikx_0} + r^{+}e^{-ikx_0} \\ U(R_2) = r^{-}e^{+ik(x_0+D)} + r^{+}e^{-ik(x_0+D)} \end{cases} \quad (1)$$

where the time and frequency dependence is omitted for convenience, k is the wavenumber, x_0 is the distance from a reference point (in this case the distance from the source), D is the

receiver spacing, $U(x)$ are the amplitudes and phases of the signal at different locations, and r^+ and r^- are the unknown amplitudes and phases of the positive and negative going waves, respectively, at the reference point. In this paper, the wave decomposition method is used with a greater number of receivers than the number of unknowns. Hence the system of equations is overdetermined and generally does not have an exact solution. In the case of *N* receivers, equation (1) becomes:

$$\begin{matrix} U(R_1) \\ U(R_2) \\ \{U(R_3)\} \\ \dots \\ U(R_N) \end{matrix} = \begin{bmatrix} e^{+ik\mathrm{x}_0} & e^{-ik\mathrm{x}_0} \\ e^{+ik(x_0+D)} & e^{-ik(x_0+D)} \\ \dots & \dots \\ e^{+ik(x_0+\mathrm{ND})} & e^{-ik(x_0+\mathrm{ND})} \end{bmatrix} \begin{Bmatrix} r^- \\ r^+ \end{Bmatrix} \tag{2}$$

It comprises a vector of *N* amplitudes, the *N*x2 matrix of constant term and the vector of the unknowns. The wavenumber k is known *a-priori* and it has a dependency on frequency. The *f-k* transformation is the common techniques to analyse seismic data coming from a MASW survey, and, since it is a well-established signal processing method for seismic data, a rigorous overview is omitted in this paper [11], [34]–[40].

Finally, the method of ordinary least square can be used to find an approximate solution that minimizes the error of the system of equations [41]. For the overdetermined system:

$$r = A_w \hat{x} \tag{3}$$

where $\hat{x}$ is the vector of the approximate solution, r is the amplitude vector, A_w the matrix of constant terms, the solution of the least square formula can be written as follows:

$$\hat{x} = (A_w^T \cdot A_w)^{-1} A_w^T \cdot r \tag{4}$$

where the matrix $(A_w^T \cdot A_w)^{-1} A_w^T$ is the Moore-Penrose inverse matrix of A_w [42].

The solution descending from (4) is complex and allows the computation of the reflection and the transmission coefficients. The phase angle of the complex solution contains the

information about the distances travelled by the direct positive going R-wave and by the negative going R-wave. The phase angle, as descending from the equation (4), is also susceptible to any phase change occurring at the boundaries and edges of the discontinuity. In the following numerical and experimental investigations, the condition number of the matrix A_w will always be close to unity (and always smaller than 5), and the signals are windowed using an exponential window, as suggested in [43].

The wave decomposition method, originally applied for simple structures and monochromatic waves, is applied here in dispersive media (road systems). For this purpose, the dispersive relationship needs to be *a-priori* information for the entire range of frequency. Dispersion is taken into account by providing the wavenumber solution of the dispersive problem, by extracting the maxima of the *f-k* spectrum of the undamaged case.

Inaccuracies in the estimation of wave caused by intrinsic attenuation and geometrical decay may also occur. For the formulations of equation (1) the geometrical decay is deliberately neglected, since taking it into account would mean the *a-priori* knowledge of the location of the crack, which is, for hypothesis, unknown. The key point of the method presented here is the use of a wave decomposition method with a significantly larger number of measurements (naturally needed to obtain the *f-k* spectrum with enough resolution) than the number of unknowns and its application to heterogeneous, dispersive materials.

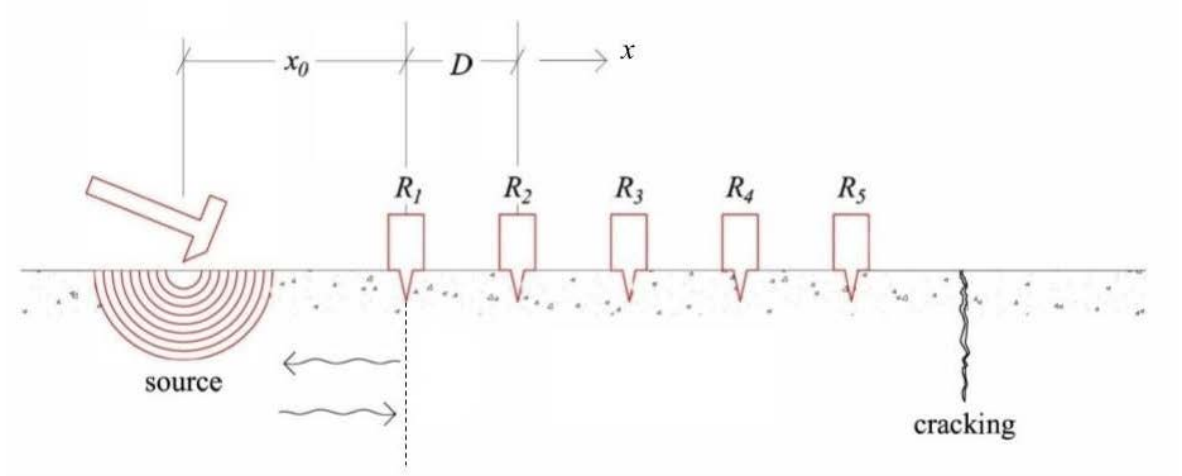

Figure 1 One-dimensional waves in the top layer of a pavement system in the presence of a discontinuity, and wave decomposition experimental set-up. *R* refers to a geophone, x_0 is the distance from a reference point, *D* is the receiver spacing.

2.1. Depth resonances of surface-breaking cracks

The resonance-type feature of surface-breaking cracks was observed by many authors [16], [19]–[21] and is associated with the depths of the cracks by the following expression [19] :

$$f_{\text{res}} \leq \frac{d \cdot V_R}{2 \cdot h} \tag{5}$$

where f_{res} is one resonant frequency, h is the depth of the vertical surface-breaking crack, d is the resonance integer index and V_R is the Rayleigh wave velocity. These frequencies correspond to resonant modes of vibrations of surface waves, propagating on the faces of the crack. Equation (5), originally derived for the half-space case [19], is shown to be applicable to layered media in this paper.

3. Numerical models

Two-dimensional finite element models of the ground are assembled through the Abaqus/CAE software to investigate the wave decomposition method in half-spaces and layered systems. The models used in this paper are semi-elliptical, with semi-major axis of 10 m and semi-minor axis of 7.5 m. Each layer is elastic and isotropic. In this paper plain-strain, finite and infinite elements are used in combination for model asphalt: a 3-node bilinear triangle (CPE3) and a 4-node bilinear quadrilater (CINPE4). Infinite elements are applied to the boundaries of the model. Following the work of Zerwer [34], since we only have interest in surface wave measurements, the mesh element size progressively increases in the downward vertical direction. The mesh elements are smaller near the surface, where Rayleigh wave propagates, with an element size l_{max} equal to 0.05 m.

Two discretization constraints have been adopted to achieve appropriate spatial and temporal resolution. The spatial condition assures that a sufficient number of points in space are sampled in order to recreate the wave, or in other word that the element size l_{max} is small enough (it is the analogue of the Nyquist's criterion in the time domain) [34], [44]. It is chosen to follow the expression:

$$f_{\text{max}} \leq \chi \frac{V_R}{l_{\text{max}}} \tag{6}$$

where V_R is the Rayleigh wave velocity, f_{max} is the maximum frequency, and χ is chosen to be 0.5 in this work.

The temporal constraint ensures that the wave front does not travel faster than the time step Δt. This is achieved by respecting the Courant-Friedrichs-Lewy condition [34], [45], [46] , here rearranged for a two-dimensional problem:

$$\Delta t_{\max} \leq \frac{1}{V_P \sqrt{\frac{1}{l_{\max^2}}}} \tag{7}$$

where V_P is the velocity of the compressional wave.

Damping is expressed as Rayleigh damping in terms of the stiffness-proportional damping [34], [45]–[47]. Stiffness-proportional damping is set in each simulation, following the work of Zerwer [28] and of Jou-Yi Shih [48], in the attempt to avoid high damping at low frequencies and the presence of extraneous numerical (parasitic) modes at the high frequencies. The model is unconstrained to avoid reflection that may occur by constraining the nodes of the finite elements.

The discontinuity is a rectangular, vertical, empty notch. It has various depth, but the width is kept constant and equal to 0.01 m in all the forthcoming simulations. Sampling frequency varies according to each simulation, which has duration $T$of 0.10 sec. Impulsive loads normal to the free surface are used to simulate the impulsive impact of a mallet with the surface. Different types of loads have been used in the forthcoming simulations, for which energy is distributed among different frequency bandwidths. Since in the forthcoming simulations the Young's modulus of the layers is progressively increased whereas the depth of the cracking is progressively decreased, loads capable of exciting a wider range of frequencies are adopted. The time histories and the auto-spectra of the loads used in the forthcoming simulations are depicted in Figure 2. A complete validation of the models used in this paper (by means of a comparison with analytical models) and pictures of its shape can be found in [49].

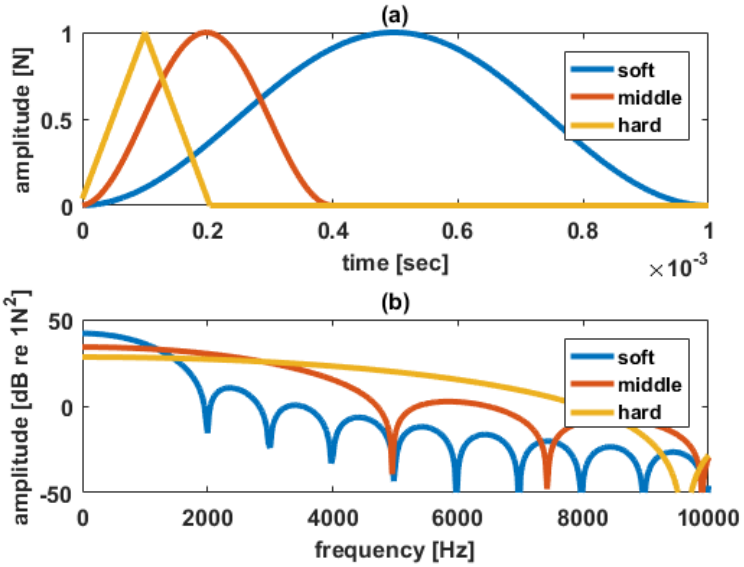

Figure 2 Time histories (a) and auto-spectra (b) of the impulsive loads used in the simulations. Load 'hard' is used for stiffer media, whereas load 'middle' and 'soft' are used for progressively softer media, as indicated in Table 1

4. Numerical investigation

The wave decomposition method is applied to data coming from four different numerical simulations of various layered systems and vertical surface-breaking discontinuities (see Table 1).

The first simulation (Model A) is performed on a half-space with low stiffness, with a large-depth crack and with no crack at all: the purpose is to check the effectiveness of the method in a non-dispersive media and to understand the resonant-type feature of surface-breaking cracks. The second simulation (Model B) is performed on the half-space with realistic parameters and with decreased cracking depths to study its effect on the reflection coefficient. Also, the deployment is moved across the crack, to estimate and study the transmission spectrum. Following simulations on two-layered, dispersive media are

performed with realistic mechanical properties, reduced crack sizing and reduced number of sensors to further approach real-life scenarios (Model C and D). Since the wave velocities are larger in models B, C and D, a different sampling frequency is chosen to respect the Courant-Friedrichs-Lewy condition (see section 3). Mechanical parameters, density and damping ratios have been chosen to be close to typical values of soils and asphalts, and are similar to those used in [22], [23], [30], [50].

	Half-spaces, non-dispersive systems				**Two-layers, dispersive systems**			
Model	A	B			C		D	
No. layers	1	1			2		2	
Thicknesses [m]	∞	∞			0.2	∞	0.2	∞
Poisson's ratio	1/3	1/3			1/3		1/3	
Density [kg m^{-3}]	2000	2000			2000		2000	
Young's modulus [MPa]	100	1000			6000	1000	2000	1000
P-wave velocity [m s^{-1}]	272	861			2108	861	1217	861
R-wave velocity [m s^{-1}]	128	405			990	405	571	405
Minimum wavelength, λ_{min} [m]	0.1	0.1			0.1	0.1	0.1	0.1
Maximum frequency, f_{max} [Hz]	1280	4050			4050		4050	
Stiffness damping	2E-5	4E-6			8E-6	2E-5	8E-6	2E-5
Load type	soft	hard			middle		middle	
Sampling frequency [kHz]	20	50			50		50	
Crack depth [m]	3.0	1.0	0.5	0.2	1.0		0.18	
Number of sensors, *N*	60	22			6		6	
Spacing between sensors, *D* [m]	0.05	0.05			0.1		0.1	

Table 1 Parameters of the FEM models for crack detection with the wave decomposition method

The reflection coefficient is computed, for all the simulations, as the amplitude ratio of the negative going wave to the positive going wave at the reference node. The transmission coefficient is computed only when the crack is across the deployment of sensors (model B, C, D). It is evaluated as the amplitude ratio of the direct positive going wave on the right end side of the notch to the direct positive going wave on the left end side of the notch, evaluated at their respective reference nodes. Table 1 shows the parameters of the FEM models used for crack detection with the wave decomposition method.

4.1. Numerical simulations on a non-dispersive half-space

In this section, the wave decomposition method is applied to numerical data coming from simulation with model A and B, i.e. non-dispersive systems. Figure 3 illustrates the set-up and the dimensions of numerical simulation with the two models. For model A, the source is 5 m distant from the deployment of sensors (Figure 3(a)). The same model is used with no crack at all. For model B, the crack is within the deployment of sensors and the source is 0.05 m far from the deployment of sensors (Figure 3(b)).

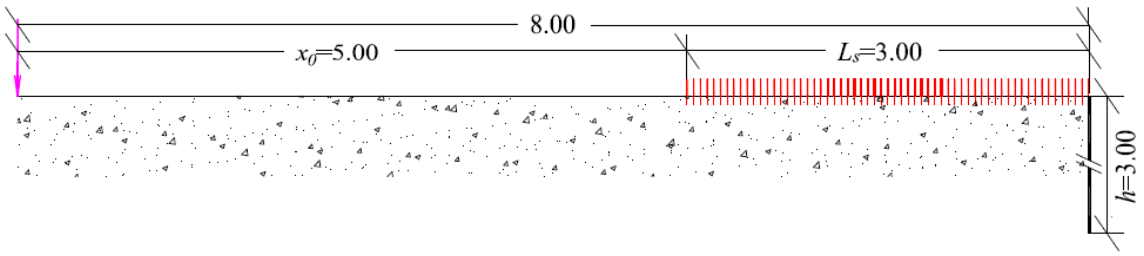

(a)

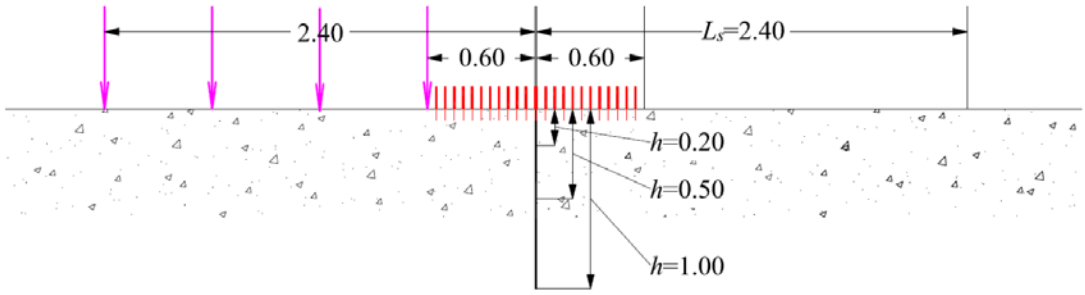

(b)

Figure 3 Set-up and dimensions for numerical simulation with model A (a) and with model B (b). The pink arrows indicate the source positions; the red lines indicate the sensors. Distances are shown in metres

Since the models are non-dispersive (i.e. the phase velocity does not depend on frequency), the *f-k* analysis is not necessary for the application of the wave decomposition method.

Figure 4(a) draws the amplitude of the direct and reflected waves at reference point, as obtained from the wave decomposition method with model A. The amplitude of the direct wave is always larger than that of the reflected wave, especially at the low frequencies (less than 300 Hz). The amplitude of both the direct and reflected R-wave at the reference point decreases moving from the low to the high frequencies due to intrinsic attenuation. Particularly, the higher frequencies at 400 Hz experience a drop in amplitude of about 100 dB with respect to the lower frequencies. Hence, it can be assumed that the signal does not contain any frequency content higher than 400 Hz and the forthcoming statements for this simulation are valid up to the aforementioned frequency.

The reflection coefficient in the presence of a discontinuity (Figure 4(c)), decreases and increases again rapidly for low frequencies, showing a major peak at the frequency of

approximately 21 Hz. Remembering equation (5), the first resonant peak is associated with the resonance index d equal to 1 and to a depth of the crack h equal to 3 m. After the major resonant peak, the reflection coefficient smoothly decreases due to the intrinsic attenuation of R-wave, with the high frequencies decaying faster than the low frequencies. Model A shows other minor peaks at the frequencies of approximately 35 Hz, 63 Hz, 102 Hz, 123 Hz, 161 Hz and 185 Hz: they are associated with the resonance indices d equal to 2, 3, 5, 6, 8, and 9. The peaks associated with the resonance indexes 4 and 7 are not visible and are probably masked in the reflection coefficient due to the solution being an approximation, or due to lack of frequency resolution. The resonant peaks are highlighted with red arrows in Figure 4(c). The image also shows the reflection coefficient in absence of a discontinuity for comparison: in this case, the reflection coefficient only decreases and rapidly approaches the zero value.

The phase of the direct and reflected R-wave, and their difference, have a linear trend up to 400 Hz and carry the information of the distance travelled by the waves with respect to the reference node (Figure 4(b)). The latter is 5 m distant from the source and 3 m distant from the discontinuity. Given the dimensions of Figure 3(a), the direct wave travels 5 m, while the negative wave travels 11 m: the phase difference gives the doubled distance between the reference sensor and the discontinuity, which in this case is 6 m. The phase of reflected waves will not be investigated on this paper as a method for crack localisation.

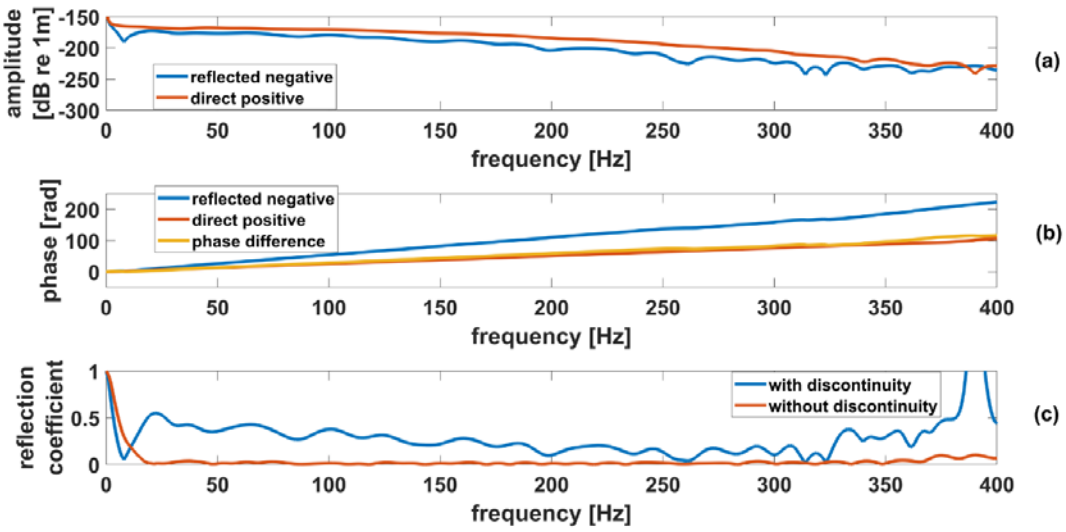

Figure 4 Amplitude (a) and phase (b) of reflected negative going and of direct positive going R-wave, and reflection coefficient of R-wave with and without discontinuity (c), for numerical simulation with model A. The amplitude of the direct and reflected waves drops by more than 100 dB in the range 0-400 Hz (a). The resonant peaks in the reflection coefficient are highlighted with red arrows (c)

Simulations with model B are presented with more realistic parameters. The asphalt properties are applied to the full half-space. For each crack depth, the wave decomposition method is applied to the deployment of sensors on the left end side of the notch to compute the reflection coefficient, and then to the deployment of sensors on the right end side of the notch to compute the transmission coefficient. Each simulation is repeated moving apart the source by an equal length L_s three times, and the reflection and transmission coefficients are a result of an average among four measurements.

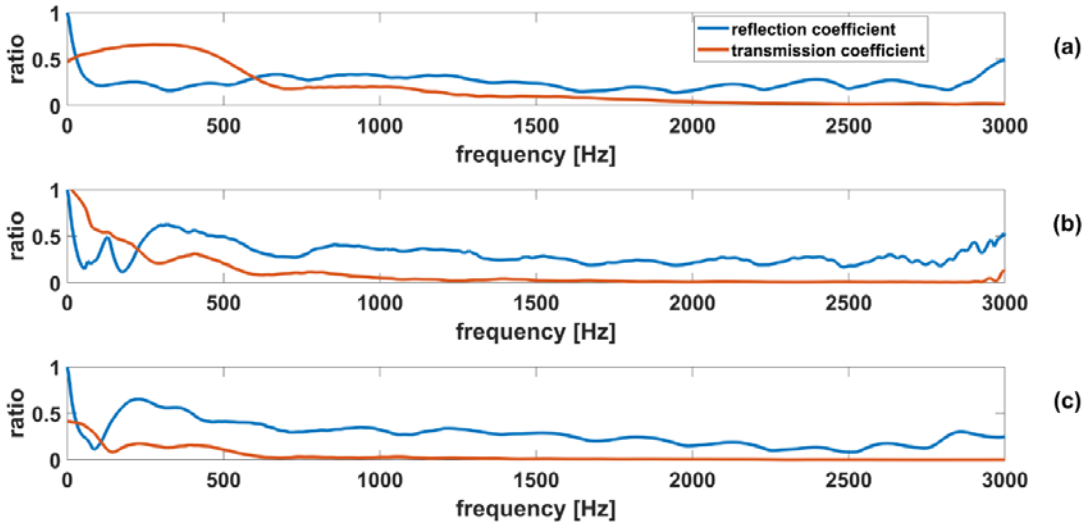

Figure 5 Reflection and transmission coefficients for the vertical crack with depth of 0.20 m (a), of 0.50 m (b) and of 1.00 m (c). The result is the average among four simulations with model B. The resonant peaks in the reflection coefficient are highlighted with red arrows

The reflection and transmission coefficients are shown in Figure 5 for three different crack depths. The reflection coefficient in all the cases shows a trend in which it firstly decreases and then increases moving from the low to the high frequencies, with one or more resonant peaks. The resonant peaks are highlighted with red arrows in Figure 5. The peaks are consistent with the resonant behaviour of surface-breaking cracks, and are associated with the depth of the crack, as per equation (5). The transmission coefficient in all the cases has a high value at low frequency, dropping down with a steep trend up to a cut-off frequency, where it approaches the zero value. Sometimes more than one cut-off is visible, with a trend in which the value of the transmission coefficient decreases and increases while tending to the zero value. This behaviour reflects the effect of a surface breaking crack on the R-wave propagation: the finite depth blocks shorter-wavelength (higher frequency) Rayleigh waves,

allowing only the longer wavelength (lower frequency) to move on, thus acting as a low-pass filter. As shown in Figure 5, the deeper the crack is, the lower the resonant and the cut-off frequencies are. Moreover, when the reflection coefficient shows a peak, the transmission coefficient shows a local minimum. Resonances and cut-offs occur approximately at the same frequency.

4.2. Numerical simulation on dispersive, layered systems

In this section, the wave decomposition method is applied to numerical data coming from simulations with dispersive, two-layered models, C and D, in the presence of a vertical discontinuity. The following simulations are performed with realistic layered systems, trying to emulate real layered systems and the set-up that will be encountered in the experimental investigations of section 5.1 and section 5.2, which employs a reduced number of sensors. The biggest challenge in the application of the wave decomposition method on layered systems is that the medium is dispersive, i.e. the phase velocity is not constant with respect to the frequency, but it varies with a specific trend due to the properties of the system. The wavenumber and phase velocity for the computation of the depth of the cracks are obtained from the extracted energy maxima of the *f-k* spectrum. In fact, phase velocity in the following numerical and experimental investigations is calculated as wavelength times its associated frequency.

Figure 6(a) and Figure 6(b) illustrates the set-up and the dimensions of numerical simulations with model C and D, respectively. The crack is in the exact middle of the deployment of sensors, equally distant from the third and the fourth sensor. In model C, the crack spans the two layers, whereas in model D the crack expands only in the first, shallowest layer. Each simulation is

repeated moving apart the source by an equal length L_s three times, and the reflection and transmission coefficients are a result of an average among four measurements. The wavenumber and phase velocity are extracted from the vertical *f-k* representation of the multichannel record on the same isotropic layered medium with absence of discontinuity, with the set-up configuration of Figure 6. Figure 7 shows the dependency from frequency of the wavenumber and of the phase velocity for the layered model C and D, as obtained from the vertical *f-k* spectra. As shown in Figure 6, four measurements are simulated to obtain a *f-k* spectrum with enough wavenumber resolution.

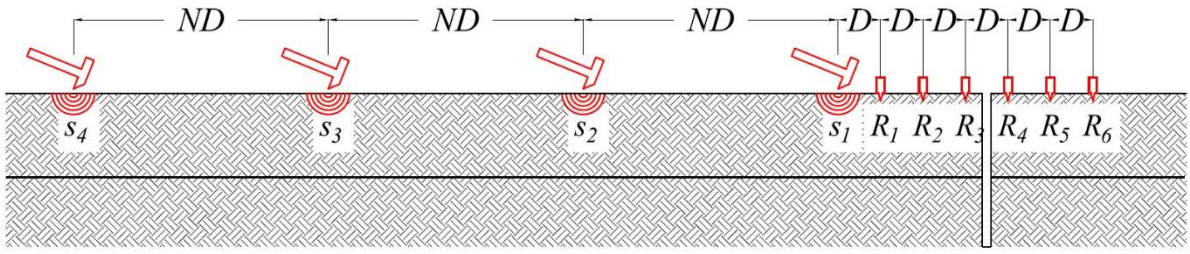

(a)

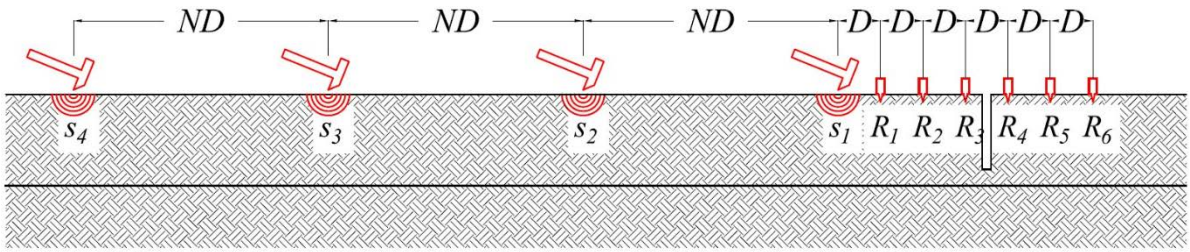

(b)

Figure 6 Set-up configuration for numerical simulations C (a) and D (b) on a two-layered system. The crack is in the exact middle of the deployment of sensors, equally distant from

the third and the fourth sensors. Crack depth is 1.00 m for model C and 0.18 m for model D. *R* refers to a geophone, *s* refers to a source, *N* is the number of receivers and *D* is the receiver spacing

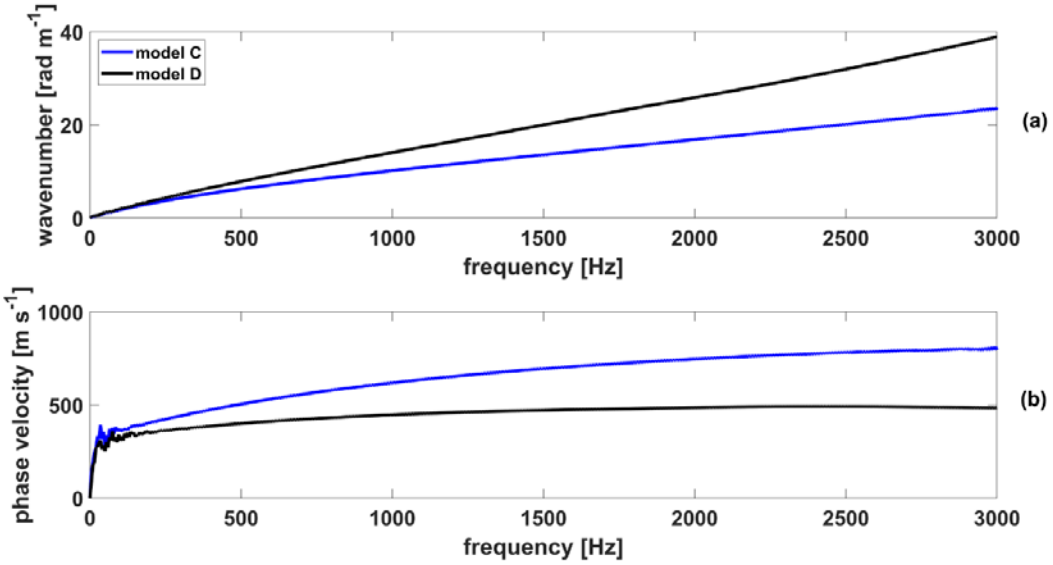

Figure 7 Wavenumber (a) and phase velocity (b) against frequency for layered model C and D, obtained from the *f-k* spectra

The reflection and transmission coefficients are shown in Figure 8 for the two simulations. They show the same behaviour observed in the numerical simulations with the half-space. For simulation with model C (Figure 8(a)) the reflection coefficient displays its first and second resonant peaks at the frequencies of approximately 190 Hz and 435 Hz. The peaks are associated with the depth of the crack and to the resonance index d respectively equal to 1 and 2, as per equation (5). They are highlighted by red arrows in Figure 8(a). Following equation (5) and assuming the phase velocity of 405 m s^{-1} and of 485 m s^{-1} from Figure 7(b), as it is obtained by dividing the frequency by its corresponding wavenumber, the first peak is associated with a crack depth of 1.06 metres and the second peak to a crack depth of 1.15

metres. The two values are consistent and very close to the actual crack depth for simulation C. The transmission coefficient for simulation C has a cut-off at the frequency of approximately 180 Hz: it occurs approximately when the reflection coefficient peaks and is again associated with the depth of the crack. The transmission coefficient than slightly increases, showing a second cut-off at the frequency of approximately 500 Hz. Cut-off frequencies of the transmission coefficient are highlighted by black arrows in Figure 8(a).

For simulation with model D (Figure 8(b)) the reflection coefficient displays its first and second resonant peaks at the frequencies of approximately 910 Hz and 2000 Hz. The peaks are associated with the depth of the crack and to the resonance index d respectively equal to 1 and 2, as per equation (5). They are highlighted by red arrows in Figure 8(b). Following equation (5) and assuming the phase velocity of 441 m s^{-1} and of 486 m s^{-1} from Figure 7(b), as it is obtained by dividing the frequency by its corresponding wavenumber, both resonant peaks are associated with a crack depth of 0.24 metres. The crack depth is very close to the actual depth, albeit it is slightly overestimated. It is also worth to notice the presence of a small hump in the reflection coefficient that shows up at approximately 200 Hz: it is probably a phenomenon associated with a mode switch in the wave propagation pattern rather than linked to the presence of the crack, since for the same value of frequency the transmission coefficient shows a high value. The transmission coefficient for simulation with model D has the first cut-off at the frequency of approximately 900 Hz: it occurs when the reflection coefficient peaks and is again associated with the depth of the crack. The transmission coefficient than slightly increases, showing a second cut-off at the frequency of approximately

1900 Hz. Cut-off frequencies of the transmission coefficient are highlighted by black arrows in Figure 8(b).

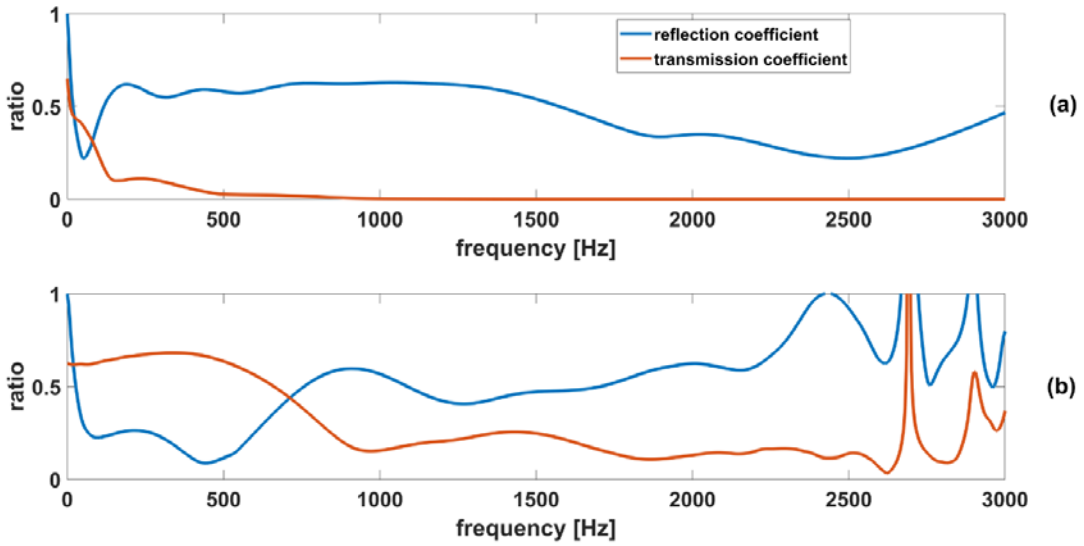

Figure 8 Reflection and transmission coefficients for model C (a) and model D (b)

Model	Resonant frequency [Hz]	Resonance index	R-wave velocity [m s^{-1}]	Estimated crack depth, h [m]	Actual crack depth [m]	Error [%]
A	21	1	128	3.00	3.00	+0
B	905	1	405	0.22	0.20	+10
	300	1	405	0.66	0.50	+32
	230	1	405	0.88	1.00	-13
C	190	1	405	1.06	1.00	+6
	435	2	485	1.15	1.00	+15
D	910	1	441	0.24	0.18	+33
	2000	2	486	0.24	0.18	+33

Table 2 Resonant frequencies, R-wave velocity, estimated and actual crack depths and relative error, for simulations with model A, B, C and D.

Table 2 summarizes the depths estimated from the resonant frequencies as per equation (5) for model A, B, C and D. The estimation of the crack depth is achieved with a lowest accuracy of 33%. The wave decomposition method demonstrated to be a reliable technique for the calculation of reflection and transmission coefficients in the presence of an anomaly or a vertical discontinuity in layered systems. It demonstrated to be able to cope with the heterogeneities and the dispersive behaviour of layered system, thus making possible to evaluate the depth of surface-breaking cracks.

5. Experimental investigations

Two experimental investigations, with the aim of applying the wave decomposition method to real situations in the presence of a discontinuity, are carried out. Previously, the wavenumber and frequency are extracted from the results of the experimental investigation

conducted on an undamaged section of the same road, which is assumed to have the same properties of the damaged section. The *f-k* spectra are obtained with a double fast Fourier Transform, as explained in [11]. Subsequently, the test is conducted with the same set-up on the damaged section of the pavement.

In the first investigation, the discontinuity is external and normal to the deployment of sensors, thus only the reflection coefficient is computed. In the second investigation the crack is across the deployment of sensors, hence both reflection and transmission coefficients are computed for the evaluation of the crack depth.

The data is acquired using a ProSig P8020 data acquisition unit. In the following experimental investigation all the tests are repeated and recorded 5 times with a sample frequency of 8 kHz and duration T of 1 sec, under the same input conditions, and then averaged in the frequency domain. For the purposes of this work, tri-axial geophones SM-24 from ION Sensor Nederland with a cut-off frequency of approximately 1 kHz have been used. In this paper, the adopted source for experimental investigations is a light mallet (0.15 kg) striking on a circular steel plate of 0.15 m of diameter and 1.5 cm of thickness, resting on the surface of the road. It has a flat frequency response up to 1 kHz (shown in [49]).

5.1. Crack external to the deployment of sensors

The wave decomposition method is applied to experimental data collected on the same road in the case of a vertical discontinuity normal to the array of sensors and in the case of absence of a vertical discontinuity. The set-up configuration is displayed in Figure 9. The vertical discontinuity is represented by the transversal edge of the asphalt, 0.10 metres distant from the array of sensors.

The vertical *f-k* representation of the seismic event for the undamaged case is shown in Figure 10 and it is used as *a-priori* information of the wave decomposition method. In the spectrum, the biggest amount of energy corresponds to the direct Rayleigh wave propagation modes and it is associated with the red bands. The black dots indicate the extracted energy maxima of the *f-k* spectrum which are directly used in the wave decomposition method, as described in section 2, and to calculate the phase velocity as the division between frequency and its corresponding wavenumber. Two outliers are present at the frequencies of 100 Hz and 300 Hz and they are discarded from the analysis. The behaviour of the propagation modes of the Rayleigh wave follows that of layered irregular systems, i.e. where the shear velocity decreases with depth. In this case, there is a very visible mode jump associated with a change in the slope at the frequency of approximately 200 Hz.

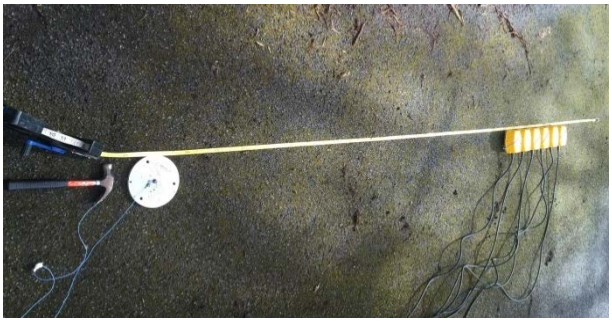

(a)

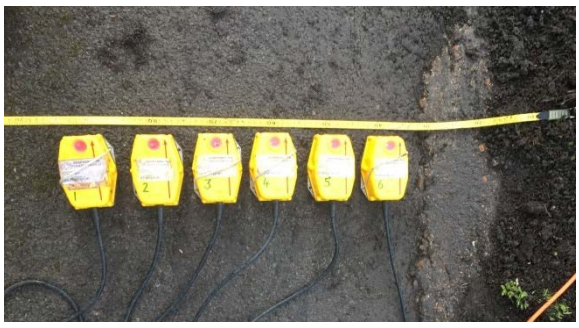

(b)

Figure 9 Experimental set-up configuration with absence of discontinuity. It is possible to observe the mallet and the aluminium plate used as a source (a). Experimental set-up configuration with the discontinuity outside the array of sensors (in this case the edge of the road pavement) (b)

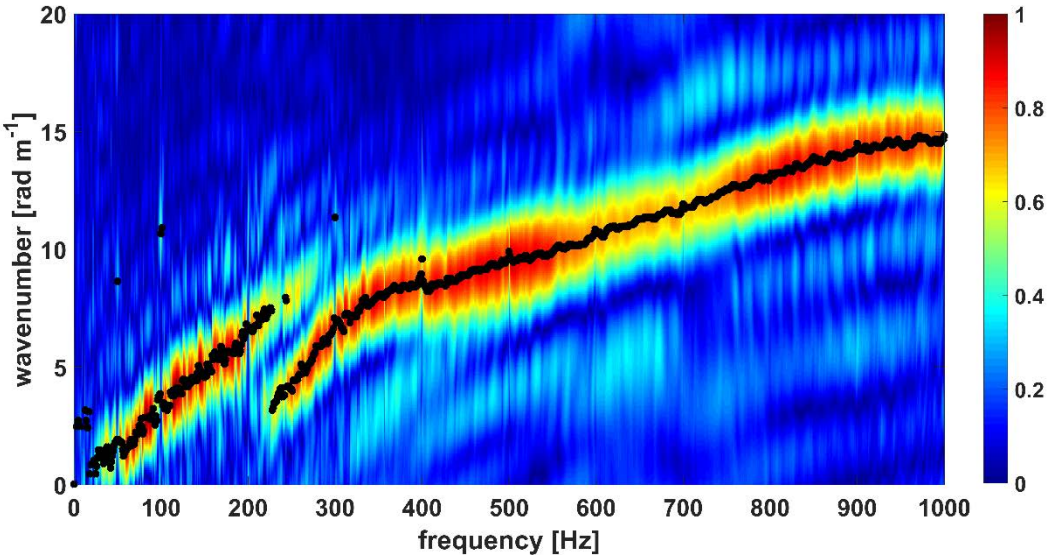

Figure 10 *f-k* spectrum of the undamaged case. The direct Rayleigh modes of propagation correspond to the red bands. The black dots indicate the extracted energy maxima of the *f-k* spectrum and are used in the wave decomposition method

The reflection coefficients obtained with and without the vertical discontinuity are displayed in Figure 11. It shows a major resonant peak at the frequency of approximately 620 Hz, when the coefficient is approximately equal to 1, and a second minor peak at approximately 220 Hz. This behaviour is consistent with the results from the numerical simulations. The resonant frequency of the reflected wave occurring at 620 Hz is associated with the crack depth whereas the first resonant peak could be associated with the mode jump that occurs at approximately 220 Hz, as it happened in the numerical simulations (see section 4.2). Bearing

in mind equation (5), if the R-wave velocity of 360 m s^{-1} and the resonance integer index d equal to 1 are assumed, the depth of the crack h is equal to 0.29 metres. The phase velocity is computed from the f-k spectrum of Figure 10, as it is obtained by dividing the frequency by its corresponding wavenumber. The depth is compatible with the total thickness of the bonded layers of the road pavement. In the absence of the crack, the reflection coefficient quickly drops to values always lower than 0.6 and remains consistent not showing relevant resonant peaks but only a small hump at approximately 230 Hz. The latter is possibly associated with the mode jump occurring in the propagation pattern (which is also visible in the spectrum of Figure 10).

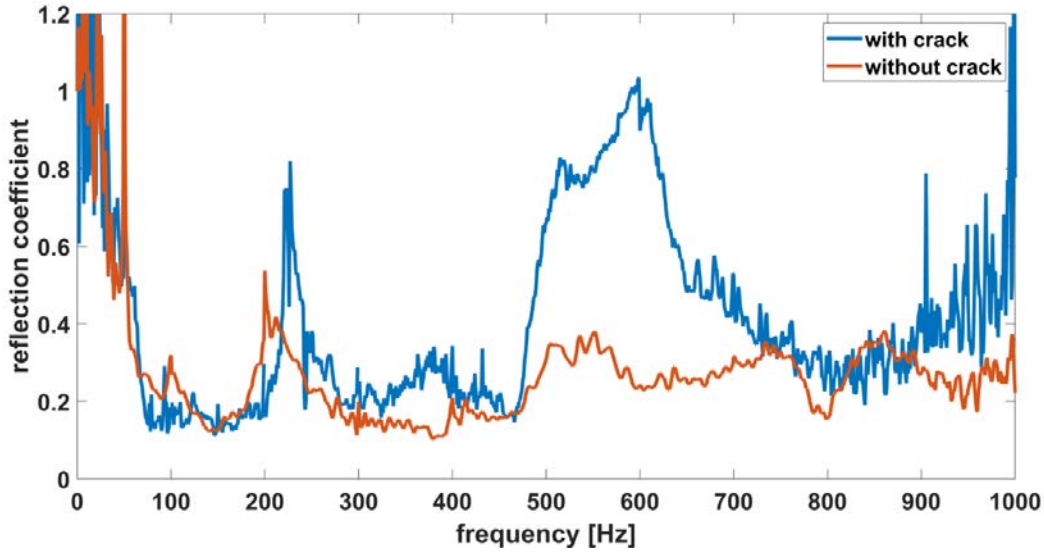

Figure 11 Reflection coefficients obtained with the wave decomposition method, cases with and without discontinuity

5.2. Crack within the deployment of sensors

A second experimental investigation is performed to assess the depth of a surface-breaking crack situated across the deployment of sensors. The set-up configuration is displayed in

Figure 6 and Figure 12. In this experimental session, a 0.01 metres wide vertical cracking in the surface is visible and symmetrically located between geophone 3 and geophone 4, internally to the geophone array.

The wavenumber and phase velocity are extracted from the results of the experimental investigation conducted in an undamaged area in the proximity of the location of this experiment. The vertical *f-k* representation of the undamaged case is shown in Figure 13 and used as a-priori information of the wave decomposition method. It displays peaks corresponding to the direct Rayleigh modes of propagation, associated with the red areas. The black dots indicate the extracted energy maxima of the *f-k* spectrum which are directly used in the wave decomposition method, as described in section 2, and to calculate the phase velocity as the division between frequency and its corresponding wavenumber. The behaviour of the propagation modes of the Rayleigh wave follows that of layered irregular systems, i.e. system where the shear velocity decreases with depth.

Figure 12 Experimental set-up configuration with the discontinuity located in the middle of the array of sensors

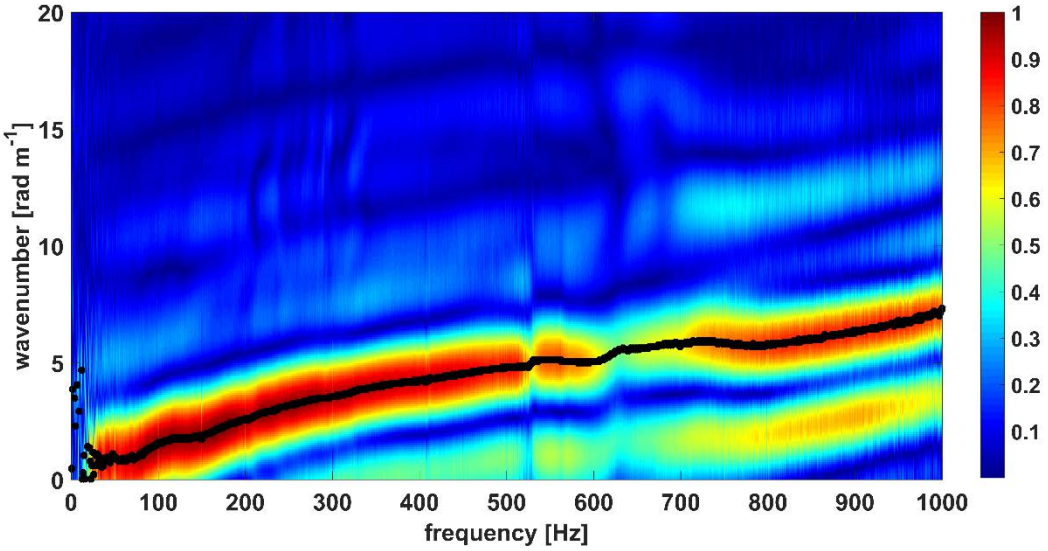

Figure 13 *f-k* spectrum of the undamaged case. The direct Rayleigh modes of propagation correspond to the red bands. The black dots indicate the extracted energy maxima of the *f-k* spectrum and are used in the wave decomposition method

The reflection and transmission coefficient obtained with the wave decomposition method are displayed in Figure 14. The reflection coefficient shows a trend in which it firstly decreases and then augments moving from the low to the high frequencies, with one major resonant peaks at approximately 200 Hz, and a second peak at 620 Hz. The peaks are associated with the depth of the crack. The transmission coefficient has a high value at the low frequencies, dropping with a steep trend up to a cut-off frequency of approximately 200 Hz, where it approaches the zero value. A second cut-off frequency is visible at approximately 580 Hz. The resonances and the cut-offs occur at the approximately the same frequencies (as in the numerical investigations of section 4.2). Bearing in mind equation (5), if the R-wave velocity

of 500 m s^{-1} and the resonance integer index d equal to 1 are assumed for the first resonant peak, the depth of the crack h is estimated to be 1.25 m. If the R-wave velocity of 725 m s^{-1} and the resonance integer index d equal to 2 are assumed for the second resonant peak, the depth of the crack h is estimated to be 1.17 m. The phase velocity is computed from the f-k spectrum of Figure 13, as it is obtained by dividing the frequency by its corresponding wavenumber. The results of the wave decomposition method indicate a very deep crack, potentially propagating all the way down to the unbound layers of the road system. They suggest a severe damage which could not be validated by destructive tests.

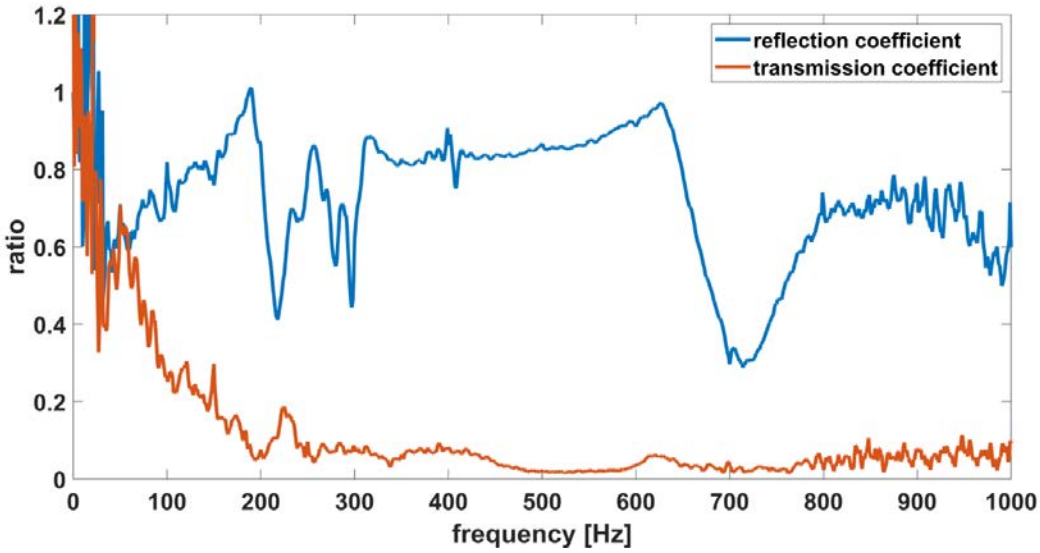

Figure 14 Reflection and transmission coefficients from wave decomposition method. The vertical discontinuity is internal to the deployment of sensors

6. Discussion

This method is intended to be a complementary add-on to non-destructive tests like the MASW, commonly used for the *in-situ* evaluation of asphalt stiffness and profiling. In fact, the wave decomposition method shares the same set-up configuration and no additional training

is required for executing the test. As it happens for the MASW, the spectrum obtained from the *f-k* analysis could be used to obtain the shear wave profiling of the road, by performing an analytical inversion of the wavefield or of the dispersion curve. The method is advantageous with respect to only MASW since the data is further analysed to obtain information on crack size.

Since the method relies on the identification of resonances in the reflection coefficient, maximum and minimum investigation depths depend on the frequency bandwidth of excitation. Care must be taken to ensure that the wanted bandwidth around the resonant frequencies is properly excited or, in other words, that the surface-breaking crack originates within the maximum and minimum investigation depths, so that that the resonance of the reflection coefficient can be properly identified. The method has the potentiality to work for the evaluation of bottom-up cracks, so long as the proper analytical model is chosen for the evaluation of the features of the crack.

Insight into practical application for detection and crack sizing in asphalt descends from the observations of the measurement shown in this paper. A possible strategy for the interrogation of cracks would be to always collect data, where possible, with the deployment across the discontinuity. This assures the estimation of both the reflection and the transmission coefficients. To avoid misinterpretation of the results of the wave decomposition (e.g. to avoid picking out a resonance due to other causes than a vertical crack), the two coefficients should be used synergistically: in fact, the transmission coefficient should present a cut-off at approximately the same value of frequency at which the resonance occurs.

Alternatively, a comparison with the results coming from an undamaged section would also be helpful at excluding misinterpretations.

The influence of the distance of the deployment of sensors from the relevant crack affects the accuracy of the depth estimation. The number of measurements taken also affects the final results of the wave decomposition method: the more measurements are taken, the more accurate the approximate solution is. Hence, a configuration which maximizes the number of sensors and minimizes the distance of the deployment from the crack has to be chosen for the best results with the wave decomposition method.

In case the location of the crack is unknown, the phase angle could help in the localisation of the crack with respect to the deployment of sensors, but at this stage a wider investigation for the evaluation of the location of bottom-up cracks using the phase of the reflected R-wave, is needed.

Compared to existing methodologies for *in-situ*, quantitative crack depth evaluation, like the one described in [23], it is faster since it does not require a comparison between different spectral images.

The initial understanding of the wave decomposition method can be cumbersome, hence the physical interpretation of the results is intended for trained users. Future developments should incorporate a straightforward interpretation of the results to facilitate the use for a broader pool.

7. Conclusions

This paper presents the wave decomposition method to estimate the depth of surface-breaking cracks in asphalt. It consists of a signal processing algorithm capable of calculating

the direct and the reflected wave's amplitudes and phase angles from the signals of an array of sensors. It employs a greater number of measurements than the number of unknowns, and it tackles the measurement errors naturally present in experimental data by finding a least square approximate solution, with the help of the pseudo-inverse matrix for overdetermined systems. Numerical simulations showed that the wave decomposition method is effective for the assessment of the depth of surface-breaking cracks in the half-space and in layered systems. Particularly, the resonances of the reflection coefficient and the cut-offs of the transmission coefficient have an inversely proportional relationship with the depth of the crack.

The experimental investigation proved that the wave decomposition method is a reliable and powerful tool for real cracks' depth interrogation and thus for condition monitoring and maintenance of roads. Generally, the wave decomposition method demonstrated to be a reliable technique for the calculation of reflection and transmission coefficients in the presence of an anomaly or a vertical discontinuity, in layered systems. Contrariwise to other techniques, it demonstrated to be able to cope with the heterogeneities and the dispersive nature of layered systems, thus making possible to detect and assess the depth of surface-breaking cracks in roads. The received experimental results show real possibilities of its application for *in-situ* diagnostic of pavements.

8. Acknowledgements

The authors gratefully acknowledge the financial support of the UK Engineering and Physical Sciences Research Council under grant EP/K021699 "Assessing the Underworld – an integrated performance model of city infrastructures".

9. Data statement

All data supporting this study are openly available from the University of Southampton repository at **http://dx.doi.org/10.5258/SOTON/xxxxx**.

References

[1] N. Ryden, “Surface wave testing of pavements.,” Lund Institute of Technology, 2004.

[2] A.I.Alliance, “Annual Local Authority Road Maintenance Survey 2017,” no. March, 2017.

[3] F. Hugo and N.-K. J. Lee, “Using Seismic Wave Propagation as a PMS Tool,” in *4th International Conference on Managing Pavements (1998)*.

[4] M. Jurado, N. Gibson, M. Celaya, and S. Nazarian, “Evaluation of Asphalt Damage and Cracking Development with Seismic Pavement Analyzer,” *Transp. Res. Rec. J. Transp. Res. Board*, vol. 2304, no. 1, pp. 47–54, 2013.

[5] D. Yuan, S. Nazarian, D. Chen, and M. McDaniel, “Use of Seismic Methods in Monitoring Pavement Deterioration During Accelerated Pavement Testing with TxMLS,” *Int. Conf. Accel. Pavement Test.*, p. 30, 1999.

[6] N. Gucunski and A. Maher, “Evaluation of Seismic Pavement Analyzer for Pavement Condition Monitoring,” *No. FHWA-NJ-2002-012*, no. May, p. 117, 2002.

[7] W.-J. Song, J. S. Popovics, J. C. Aldrin, and S. P. Shah, “Measurement of surface wave transmission coefficient across surface-breaking cracks and notches in concrete,” *J. Acoust. Soc. Am.*, 2003.

[8] S. Nazarian, M. R. Baker, and K. Crain, “Development and Testing of a Seismic Pavement Analyzer,” *Tech. Rep. SHRP-H, 375.*, 1993.

[9] S. Lin, J. C. Ashlock, and R. C. Williams, “Nondestructive quality assessment of asphalt pavements based on dynamic modulus,” *Constr. Build. Mater.*, 2016.

[10] L. V. Socco, S. Foti, and D. Boiero, “Surface-wave analysis for building near-surface velocity models — Established approaches and new perspectives,” *Geophysics*, vol. 75, no. 5, pp. 75A83-75A102, 2010.

[11] C. B. Park, R. D. Miller, and J. Xia, “Multichannel analysis of surface waves,” *Geophysics*, vol. 64, no. 3, pp. 800–808, 2002.

[12] P. E. L.D. Olson and P. K. Miller, “Multiple Impact Surface Waves (MISW) – Improved Accuracy for Pavement System Thicknesses and Moduli vs. Spectral Analysis of Surface Waves (SASW),” in *ASCE GeoFlorida 2010 proceedings*, 2010, vol. 2, p. 210.

[13] R. Fedele, F. G. Praticò, R. Carotenuto, and F. G. D. Corte, “Structural health monitoring of pavement assets through acoustic signature,” in *Bearing Capacity of Roads, Railways and Airfields - Proceedings of the 10th International Conference on the Bearing Capacity of Roads, Railways and Airfields, BCRRA 2017*, 2017.

[14] S. W. Shin, J. Zhu, J. Min, and J. S. Popovics, “Crack depth estimation in concrete using energy transmission of surface waves,” *ACI Mater. J.*, vol. 105, no. 5, pp. 510–516, 2008.

[15] M. Hirao, H. Fukuoka, and Y. Miura, “Scattering of Rayleigh surface waves by edge cracks: Numerical simulation and experiment,” *J. Acoust. Soc. Am.*, vol. 72, no. 2, pp. 602–606, 2005.

[16] A. Fahr and W. R. Sturrock, “Detection and Characterization of Surface Cracks Using Leaky Rayleigh Waves,” *Rev. Prog. Quant. Nondestruct. Eval. Springer*, pp. 559–568, 1985.

[17] L. Khazanovich, R. Velasquez, and E. Nesvijski, “Evaluation of Top-Down Cracks in Asphalt Pavements by Using a Self-Calibrating Ultrasonic Technique,” *Transp. Res. Rec. J. Transp. Res. Board*, vol. 1940, no. May 2016, pp. 63–68, 2007.

[18] S. Underwood and Y. R. Kim, “Determination of Depth of Surface Cracks in Asphalt Pavements,” *Transp. Res. Rec. J. Transp. Res. Board, 143-149.*, no. November 2002, 2003.

[19] S. Ayter and B. A. Auld, “On the Resonances of Surface Breaking Cracks,” *Proc. DARPA/AFML Rev. Prog. Quant. NDE, July1978– Sept. 1979*, no. September 1979, pp. 394–492, 1980.

[20] V. Domarkas, B. T. Khuri-Yakub, and G. S. Kino, “Length and depth resonances of surface cracks and their use for crack size estimation,” *Appl. Phys. Lett.*, vol. 33, no. 7, pp. 557–559, 1978.

[21] D. A. Mendelsohn, J. D. Achenbach, and L. M. Keer, “Scattering of elastic waves by a surface-breaking crack,” *Wave Motion*, vol. 2, no. 3, pp. 277–292, 1980.

[22] N. Gucunski, P. Shokouhi, and A. Maher, “Detection and Characterization of Cavities Under the Airfield,” *NDT - Competence Saf. MATEST*, no. April, pp. 151–161, 2004.

[23] M. Iodice, J. M. Muggleton, and E. Rustighi, “Exploiting spectral differences between two acoustic imaging methods for the in situ evaluation of surface-breaking cracks in asphalt,” *Appl. Acoust.*, 2019.

[24] A. Zerwer, M. A. Polak, and J. C. Santamarina, “Effect of Surface Cracks on Rayleigh Wave Propagation: An Experimental Study,” *J. Struct. Eng.*, 2002.

[25] G. Hevin, O. Abraham, H. Pedersen, and M. Campillo, “Characterisation of surface cracks with Rayleigh waves: a numerical model,” *NDT E Int.*, vol. 31, no. 4, pp. 289–297, 1998.

[26] J. D. Achenbach, I. N. Komsky, Y. C. Lee, and Y. C. Angel, “Self-calibrating ultrasonic technique for crack depth measurement,” *J. Nondestruct. Eval.*, vol. 11, no. 2, pp. 103–108, 1992.

[27] S. H. Kee and J. Zhu, “Using air-coupled sensors to measure depth of a surface-breaking crack in concrete,” *AIP Conf. Proc.*, vol. 1096, pp. 1497–1504, 2009.

[28] A. Zerwer, M. A. Polak, and J. C. Santamarina, “Rayleigh wave propagation for the detection of near surface discontinuities: Finite element modeling,” *J. Nondestruct. Eval.*, 2003.

[29] E. Nesvijski and M. Marasteanu, “Wavelet Transform and Its Applications to Acoustic Emission Analysis of Asphalt Cold Cracking,” *E J. NDT*, 2007.

[30] M. Iodice, J. Muggleton, and E. Rustighi, “The Detection of Vertical Cracks in Asphalt Using Seismic Surface Wave Methods,” *J. Phys. Conf. Ser.*, vol. 744, no. 1, 2016.

[31] D. G. Aggelis and T. Shiotani, “Surface wave dispersion in cement-based media: Inclusion size effect,” *NDT E Int.*, vol. 41, no. 5, pp. 319–325, 2008.

[32] J. M. Muggleton, M. J. Brennan, and P. W. Linford, “Axisymmetric wave propagation in fluid-filled pipes: Wavenumber measurements in in vacuo and buried pipes,” *J. Sound Vib.*, vol. 270, no. 1–2, pp. 171–190, 2004.

[33] B. R. Mace and C. R. Halkyard, “Time domain estimation of response and intensity in beams using wave decomposition and reconstruction,” *J. Sound Vib.*, vol. 230, no. 3, pp. 561–589, 2000.

[34] A. Zerwer, G. Cascante, and J. Hutchinson, “Parameter Estimation in Finite Element Simulations of Rayleigh Waves,” *J. Geotech. Geoenvironmental Eng.*, 2002.

[35] C. B. Park, R. D. Miller, and J. Xia, “Multimodal Analysis of High Frequency Surface Waves,” in *Symposium on the Application of Geophysics to Engineering and Environmental Problems 1999. Society of Exploration Geophysicists*, 1999.

[36] T. Forbriger, “Inversion of shallow-seismic wavefields: I. Wavefield transformation,” *Geophys. J. Int.*, vol. 153, no. 3, pp. 719–734, 2003.

[37] S. Foti, R. Lancellotta, L. V. Socco, and L. Sambuelli, “Application of Fk Analysis of Surface for Geotechnical Characterization,” in *International Conferences on Recent Advances in Geotechnical Earthquake Engineering and Soil Dynamics*, 2001.

[38] S. Foti, S. Parolai, D. Albarello, and M. Picozzi, “Application of Surface-Wave Methods for Seismic Site Characterization,” *Surv. Geophys.*, 2011.

[39] A. Zerwer, “Near Surface Fracture Detection in Structural Elements Investigation Using Rayleigh Waves,” University of Waterloo, 1999.

[40] G. Das, “A Brief Review on Different Surface Wave Methods and Their Applicability for Non- Destructive Evaluation of Pavements,” *Nondestruct. Test. Eval.*, pp. 337–350, 2008.

[41] D. C. Spencer, “Overdetermined systems of linear partial differential equations,” *Bull. Am. Math. Soc.*, 1969.

[42] R. Penrose, “A generalized inverse for matrices,” *Math. Proc. Cambridge Philos. Soc.*, 1955.

[43] B. Fladung, “Windows Used for Impact Testing,” in *Proceedings of the IMAC XV*, 1997.

[44] R. L. Kuhlemeyer and J. Lysmer, “Finite element method accuracy for wave propagation problems,” *J. Soil Mech. Found. Div.*, 1973.

[45] C. T. Schröder and W. R. Scott, “A finite-difference model to study the elastic-wave interactions with buried land mines,” *IEEE Trans. Geosci. Remote Sens.*, vol. 38, no. 4 I, pp. 1505–1512, 2000.

[46] C. T. Schröder, “On the interaction of elastic waves with buried land mines: an investigation using the finite-difference time-domain method,” Georgia Institute of Technology, 2001.

[47] E.L.Wilson, *Static and Dynamic Analysis of Structures*. 2004.

[48] J.-Y. Shih, D. Thompson, and A. Zervos, “Assessment of Track-Ground Coupled Vibration Induced by High-Speed Trains,” *21st Int. Congr. Sound Vib.*, no. July, pp. 13–17, 2014.

[49] M. Iodice, “Road and Soil Dynamic Characterization From Surface Measurements,” University of Southampton, 2017.

[50] M. O. Al-Hunaidi, “Nondestructive evaluation of pavements using Spectral analysis of surface waves in the frequency wave-number domain,” *J. Nondestruct. Eval.*, vol. 15, no. 2, pp. 71–82, 1996.